

PHYSICAL REVIEW B

CONDENSED MATTER

THIRD SERIES, VOLUME 48, NUMBER 18

1 NOVEMBER 1993-II

Uniaxial-stress dependence of the phonon behavior in the premartensitic phase of $\text{Ni}_{62.5}\text{Al}_{37.5}$

S. M. Shapiro

Department of Physics, Brookhaven National Laboratory, Upton, New York 11973

E. C. Svensson

AECL Research, Chalk River Laboratories, Chalk River, Ontario, Canada K0J 1J0

C. Vettier

Institute Laue Langevin, 156X, 38042 Grenoble, France

B. Hennion

Laboratoire Léon Brillouin, 91190 Gif-sur-Yvette, France

(Received 27 January 1993)

Results of neutron-scattering experiments on a single crystal of $\text{Ni}_{62.5}\text{Al}_{37.5}$ as a function of uniaxial stress and temperature are reported. Emphasis is placed on the behavior of the low-energy part of the $[\zeta\zeta 0]$ - TA_2 phonon branch and its associated central peak. The dip in the phonon-dispersion curve is stress dependent and shifts from $\zeta=0.14$ for zero stress to $\zeta=0.18$ for an applied stress of 85 MPa at room temperature. As the temperature decreases the satellite shifts further, the phonon energy decreases considerably, and the linewidths become broad. These results are interpreted in terms of Clapp's localized soft-mode theory of nucleation in martensite.

INTRODUCTION

Martensitic transformations (MT) can be described as diffusionless (meaning no atom-by-atom rearrangement), displacive (meaning small cooperative motions of atoms) transitions which alter the symmetry but without changing the composition or order.^{1,2} The low-temperature or product phase is always a lower symmetry than the high-temperature or parent phase. Nearly all MT are first order with some being weakly first order where the properties change nearly continuously and precursor effects are present. Others are strongly first order and the transition occurs abruptly without any premonitory effects. In the latter case there is a large temperature range of coexistence of the parent and product phase. Shearlike displacements play an important role in the martensitic transformations. This is shown in studies of the elastic constants³ and phonon-dispersion curves where transverse modes behave in an anomalous way.⁴ For example, on cooling, the elastic constant of the transverse-acoustic (TA) branch decreases in value instead of the normal increase expected due to the lattice getting stiffer. Coupled to the shear response is often a "shuffle" which is a coordinated motion of atoms within a unit cell. This manifests itself as an anomaly in the TA branch at a finite wave vector.⁴⁻⁸ Thus within a martensitic transforma-

tion a $q \sim 0$ anomaly⁹ is associated with the elastic constants and a $q \neq 0$ anomaly associated with the shuffle.¹⁰

Since all MT are first order, nucleation and growth play an important role. If one uses classical nucleation theory, which involves balancing the chemical driving force, the interfacial energy, and the strain energy,¹¹ the critical size obtained is much larger than has been observed. Olsen and Cohen have taken into account the influence of defects on the nucleation with some success in predicting critical sizes.¹² Clapp and co-workers several years ago combined the soft-mode theory of phase transitions and the presence of defects in proposing the localized soft-mode (LSM) model for martensitic nucleation.^{13,14} The soft-mode theory, successfully applied to other displacive transitions such as ferroelectrics, has also been used to describe martensitic phase transformation, especially in the case of thermoelastic martensite. However, except for a few cases (Nb_3Sn , In-Tl), a mode never becomes completely soft. Clapp focuses on this idea and claims that around a defect a particular combination of stresses and strains can cause a lattice vibrational mode to soften significantly in the region near the defect and serves as a center for nucleation.¹³ Thus, a key experimental piece of information needed is the behavior of the phonon-dispersion curve as a function of applied stress. In this paper we report on such a study on

a well characterized single crystal of $\text{Ni}_x\text{Al}_{1-x}$.

$\text{Ni}_x\text{Al}_{1-x}$ alloys exhibit a MT for $60 < x < 64$ at. % with $T_M > 0$ K.¹⁵ For $T > T_M$ the structure is a cubic-CsCl-type where the excess Ni is randomly distributed over the Al sites. The temperature-composition diagram has been extensively studied and there exist several different low-temperature structures depending upon the composition.¹⁶ The precise boundary between them, however, is not well known. In addition, the T_M measured by different laboratories¹⁷ can vary by more than 100 K. One of the more extensively studied compositions,⁸ $x = 62.5$ at. %, exhibits a MT at $T \approx 85$ K and the low-temperature structure is established to be a $7M$ monoclinic phase¹⁸ with symmetry $P2/m$.

Precursors to the $7M$ martensitic transformation have been observed. The elastic constant $C' = 1/2(C_{11} - C_{12})$ show an anomalous softening³ over a 200-K temperature range above T_M . The electron-diffraction studies revealed anomalous diffuse scattering along the $[110]$ transverse directions⁸ and its image shows the distinct tweed pattern observed above T_M in many alloys exhibiting MT.¹⁹ Inelastic neutron studies can separate the relative contributions to the diffuse scattering from the phonons and the elastic diffuse intensity. These studies revealed a remarkable feature in the $[110]$ -TA₂ phonon branch.⁷ This mode corresponds to propagation along $[110]$ with displacements along $[1\bar{1}0]$ and in the long-wavelength limit, i.e., $q \rightarrow 0$, the slope of the dispersion curve corresponds to the elastic constant $C' = 1/2(C_{11} - C_{12})$. In almost all β phase materials this branch exhibits anomalous properties and, as Zener noted long ago, can lead to instabilities in the structure.²⁰ Also, the sliding of the $\{110\}$ planes associated with this mode determines the various stacking sequences of the martensitic phases such as $3R$, $9R$, $18R$, etc. In the present case where the low-temperature structure is $7M$, a "dip" in the dispersion curve is observed near $\zeta \sim 1/7$, which becomes more pronounced as T_M is approached.⁸ The mode, however, never completely softens when the martensitic temperature is approached. At the same wave vector an elastic central peak occurs whose intensity increases dramatically as $T \rightarrow T_M$. These observations clearly point to the importance of premartensitic behavior in the NiAl alloy.

In the experiment reported here we present results of inelastic neutron-scattering experiments on $\text{Ni}_{62.5}\text{Al}_{37.5}$ as a function of uniaxial stress and temperature. Emphasis is placed on the behavior of the $[\zeta\zeta 0]$ TA₂ branch and its associated central peak. The major result is that the dip in the phonon-dispersion curve moves from $\zeta = 0.14$ for zero stress to $\zeta = 0.18$ for an applied stress of 85 MPa at room temperature. As the temperature is lowered the phonon energy decreases considerably and at $T = 250$ K the phonon linewidth is very broad and the energy is near zero. These observations are interpreted as an inhomogeneous softening prescribed by the local soft-mode theory of Clapp.¹³

EXPERIMENT

The neutron-scattering experiments were performed at the Laboratoire Léon Brillouin (LLB), Saclay, France, us-

ing the Orphée Research Reactor and at the NRU reactor at the AECL Research (AECL) in Chalk River, Ontario. The key element in this experiment was the stress apparatus. For the experiments at AECL a simple clamp device was constructed which consisted of a screw squeezing upon a crystal mounted in a jig. The stress was not calibrated and a qualitative measure of it was the torque applied to the screw. Once the stress was applied the entire jig could be mounted in a closed cycle displacer refrigerator and the sample cooled. At LLB, the stress apparatus had been used in other experiments²¹ and provided a calibrated control of the applied force and, knowing the cross sectional area of the sample (5×5 mm²), the stress is determined. It could be inserted into an ILL "orange" cryostat so that the stress and temperature could be varied. The maximum applied load is 1000 kg which corresponds to an applied stress of $\sigma = 4000$ kg/cm² (392 MPa). Because of the large thermal mass of this stress cell it took considerable time for the system to thermally equilibrate once the temperature was changed.

Triple-axis spectrometers were used at both reactors ($N5$ at AECL and $1T$ at LLB) with a fixed final energy ($E_f = 14.7$ meV) used for most of the measurements. For some higher-energy phonon measurements a fixed final energy of 30.5 meV was used. At both reactors a flat PG (002) analyzer was used and at LLB a focusing PG (002) monochromator and filter were used whereas at AECL, Si (111) was used to monochromate the beam. This had the disadvantage that the intensity was considerably less (nearly a factor of 5 as determined by a standard phonon), but had the advantage that no filter is needed and any incident/final energy could be used in a scan. The energy resolution, as determined by the incoherent scattering was comparable at both reactors, $dE \approx 0.8$ meV.

The sample was the same $5 \times 5 \times 5$ mm³ cube used in previous neutron-scattering experiments.⁸ Each face is parallel to a $[100]$ direction. The lattice parameter at room temperature is 2.86 Å and the mosaic at the start of the experiment was $< 10'$, but after the first experiment at Chalk River had increased to $\approx 20'$. The crystal was oriented with $[001]$ perpendicular to the scattering plane and this was the direction of the applied stress. The phonon measurements were performed around the $(1,1,0)$ Bragg peak and the elastic scattering measured also around the $(2,0,0)$ reciprocal-lattice vector. In this case the $[110]$ direction makes an angle of 45° to the $[100]$ direction and the effects of the crystal mosaic are avoided.

RESULTS

Figure 1(a) shows the lattice parameter as a function of applied stress measured at LLB at room temperature. At AECL, where only the applied torque was measured, a linear curve of lattice parameter vs torque was also obtained. If the two curves are normalized at zero stress to account for differences in instrument calibration, and since the two curves must have the same slope, the lattice parameter can be used to calibrate the stress apparatus

for the AECL measurements. The solid circles are the lattice parameters obtained at AECL.

There is an increase in the lattice parameter as the stress is increased which is expected, since we are compressing along the [001] direction and this should cause the $\langle 100 \rangle$ directions perpendicular to the direction of the applied stress to expand. By placing the stress direction in the scattering plane we also confirmed that the lattice parameter measured along the direction of the applied stress decreases with σ such that the volume remains constant. The strain associated with the applied stress is nearly 1% over the region of applied stress. The crystal does not permanently deform in that when the stress is removed the room-temperature lattice parameter is obtained and on increasing σ the same curve is reproduced.

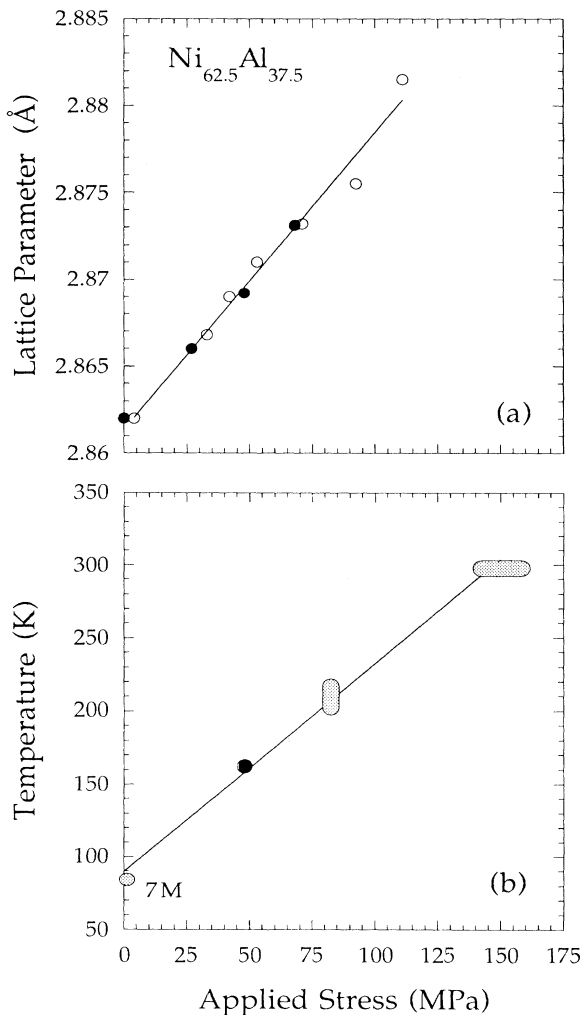


FIG. 1. (a) Lattice parameter vs stress for $\text{Ni}_{62.5}\text{Al}_{37.5}$. The open circles were measured at LLB and the solid circles were obtained at AECL. The two sets of measurements were normalized at zero stress. (b) Temperature-stress diagram for $\text{Ni}_{62.5}\text{Al}_{37.5}$. The hatched area at 300 K was determined by varying the stress whereas the point around 200 K was obtained by varying temperature. The solid circle was determined with constant stress in the clamp device.

Figure 1(b) is the stress-temperature phase diagram determined at LLB. When the transition occurred there was an abrupt change of the lattice parameter and the crystal mosaic. The value at $\sigma=0$ was obtained from earlier measurements. The solid circle is a point measured at AECL and determined by a large increase in the satellite intensity. The good agreement with the LLB data assures us that the calibration method we used for the clamp device is reasonable. The curve is linear with a slope of 1.4 K/MPa.

The next part of the experiment consisted of measuring the effects of stress and temperature on the anomalous phonon branch, the $[\zeta\zeta 0]$ - TA_2 branch and its associated diffuse scattering. This branch corresponds to propagation along $\langle 110 \rangle$ with atomic displacements along $\langle 1\bar{1}0 \rangle$. In the limit $\zeta \rightarrow 0$ the slope of this branch corresponds to the elastic constant C' . Figure 2 shows the low-energy portion of the dispersion curve of this branch. The solid circles represent the room temperature, low-stress behavior. Earlier zero-stress measurements⁸ observed that as one cools, a dip develops at $\zeta \approx 0.16$ as shown by the dotted curve. Remarkably, when the stress is applied along [001], perpendicular to the phonon direction, the anomaly deepens and shifts to larger wave vectors as seen in the dot-dashed curve. In addition, the entire dispersion curve shows a decrease in energy with increasing stress. On reducing the temperature the branch softens further and the anomaly shifts again to a larger wave vector. Figure 3 shows the neutron spectra for two wave vectors, $\zeta=0.16$ and $\zeta=0.20$. The former corre-

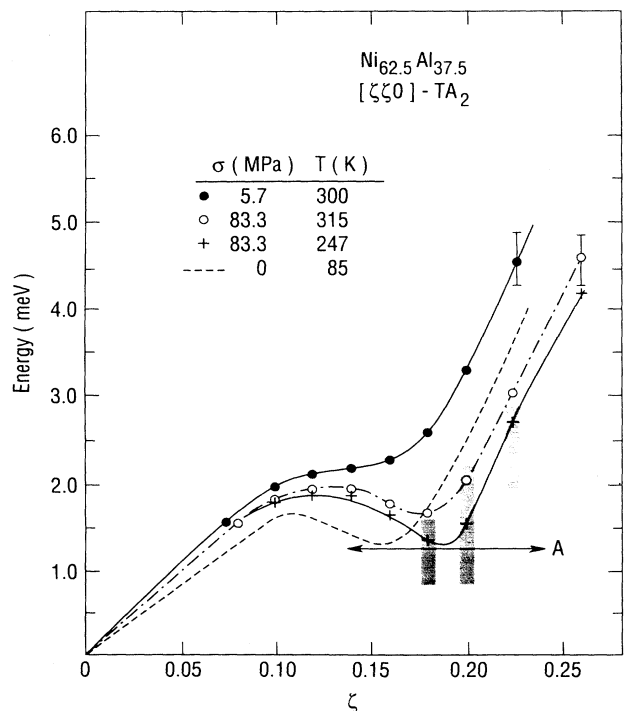


FIG. 2. The low-energy portion of the $[\zeta\zeta 0]$ - TA_2 dispersion curve for $\text{Ni}_{62.5}\text{Al}_{37.5}$. The vertical hatched area corresponds to the widths. The line marked A is the direction of the constant E scan in Fig. 4.

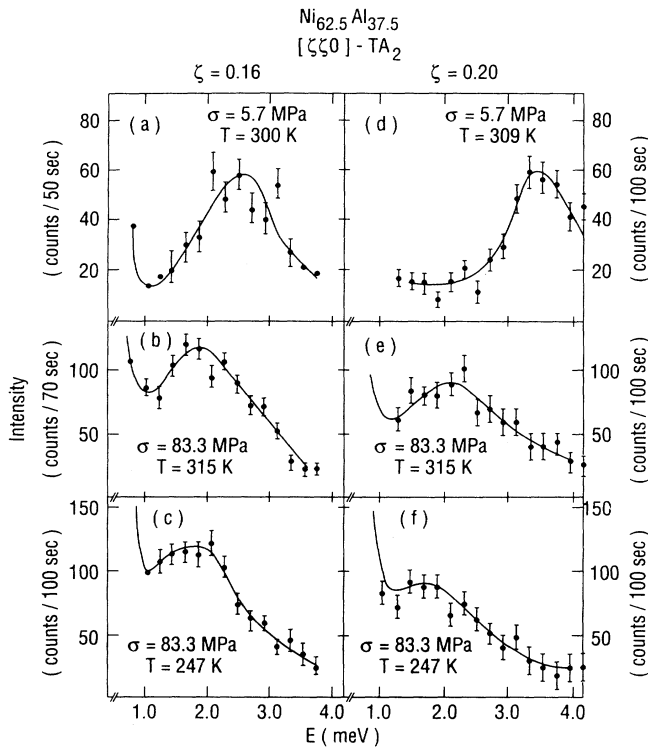


FIG. 3. Temperature and stress dependence of the spectra of several $[\zeta\zeta 0]$ - TA_2 modes in $Ni_{62.5}Al_{37.5}$. (a)–(c): $\zeta=0.16$; (d)–(f): $\zeta=0.20$.

sponds to the soft wave vector of the zero-stress measurements. There is a clear softening when a stress is applied near room temperature, but hardly any change on cooling. The softening is more dramatic for $\zeta=0.20$. Not only does the mode soften by almost 50%, but its linewidth also increases. At the lower temperatures, a

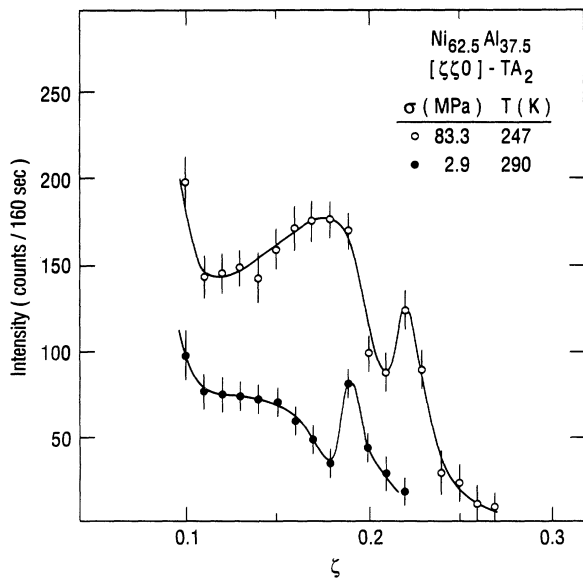


FIG. 4. Constant $\Delta E=1.25$ -meV scans along the $[\zeta\zeta 0]$ direction marked by A in Fig. 2.

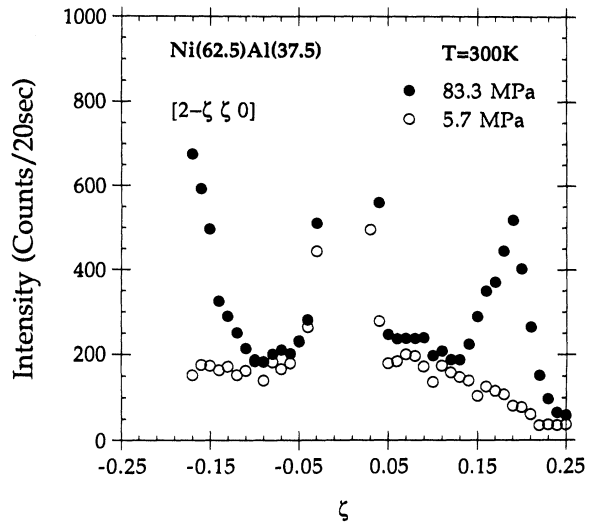


FIG. 5. Elastic ($\Delta E=0$) scans along the $[\zeta\zeta 0]$ direction through the $(2,0,0)$ Bragg peak at $T=300$ K for (\circ) 5.7 MPa and (\bullet) 83.3 MPa.

peak is hardly discernible. The hatched region in the dispersion curve of Fig. 2 corresponds to the observed linewidths. The softening is also demonstrated in Fig. 4 where constant energy ($\Delta E=1.25$ meV) scans along the $[\zeta\zeta 0]$ direction were performed. The sharp peak is part of the strong elastic scattering of a piece of the crystal that had already transformed as observed in an elastic scan. At nearly ambient conditions there is a broad shoulder near $\zeta\sim 0.15$, while at an applied stress and lower temperatures the signal has increased and a peak is present at $\zeta\sim 0.18$. This is consistent with the shift in ζ and decrease in energy with stress.

The elastic intensity also increases with stress and temperature. Figure 5 shows the elastic scattering measured along the $[\zeta\zeta 0]$ direction about the $(2,0,0)$ reciprocal-lattice vector. For the lowest stress at room temperature there is a weak maximum at $\zeta\approx 0.15$ which is identical to what was observed in earlier experiments at $\sigma=0$. On

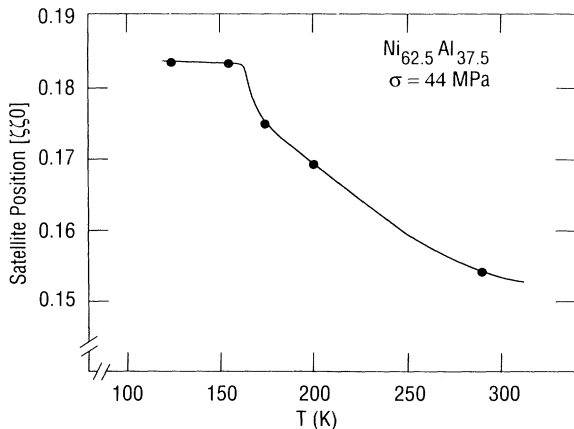


FIG. 6. Temperature dependence of satellite position along the $[\zeta\zeta 0]$ direction in $Ni_{62.5}Al_{37.5}$ for an applied stress of 44 MPa.

application of a uniaxial stress a more pronounced peak develops and its position shifts to a larger wave vector, $\xi \approx 0.18$. Figure 6 shows the stress dependence of the central peak position measured at AECL for room temperature. Its position changes on cooling as shown in Fig. 6 for an applied stress of 44 MPa. For this stress, the satellite position increases smoothly to a larger value and at the transition temperature $T_{M\sigma} \sim 150$ K it apparently saturates at $\xi = 0.18$ which is near the position of the phonon anomaly at this stress. For larger stress the satellite shifted to even larger values as seen in Fig. 5.

DISCUSSION

The first study of Ni-Al with a uniaxially applied stress was performed by Martynov *et al.*²² on a sample with a composition of $x = 63.1$ at. %. T_M ($\sigma = 0$) for this composition is reported to be 253 K. Instead of a compressive stress, Martynov used a tensile stress and studied the structure at room temperature. He was able to induce a transformation at $\sigma = 70$ MPa, which is less than reported here, but is reasonable when the differences in composition and T_M is taken into account. From Fig. 1, Young's modulus, which is the ratio of the stress to the strain, for a [001] compressive stress can be calculated. We obtain the value $Y = 1.6 \times 10^4$ MPa (or 1.6×10^{10} N/m²), which is slightly larger than the value 1×10^4 MPa obtained by Martynov *et al.*²²

The most significant result is the movement of the minimum in the dispersion curve and the shift of the satellite position with applied stress. Recently, Zhao and Harmon²³ calculated the modification of the phonon-dispersion curves of $\text{Ni}_x\text{Al}_{1-x}$ due to the electron-phonon interaction. In their calculations, the increase in x is taken into account by a lowering of the Fermi level. They were able to reproduce the experimental observation of the decrease of the wave vector of the phonon anomaly Q_{\min} as x increases. Since the present observation shows that Q_{\min} increases with applied stress, it can be concluded that by squeezing the crystal the Fermi level is raised relative to the zero-stress situation.

It is useful to compare our results with other measurements on the stress induced martensite (SIM) for Ni-Al alloys. As mentioned above Martynov *et al.*²² used a tensile stress (i.e., they "pulled" on a thin wire) in order to study the phase diagram and the stress-induced structure. They showed that with a tensile stress the $7M$ structure first forms and at a later stage the final product phase is $3R$ martensite. Recently Schryvers and Tanner²⁴ used high-resolution electron microscopy to study the SIM in $\text{Ni}_{62.5}\text{Al}_{37.5}$, the same composition studied here. They relied on a sharp tip of a microcrack, which was produced during the electropolishing of their thin foil, to give them a distribution of stresses near the crack tip. By focusing their electron beam at different distances from the crack tip they could look at different stress regions, since the stress decreases with distance from the crack tip. The value of the stresses are totally unknown but the relative magnitudes are related to the inverse of the distance from the crack. Very near the crack tip, in the region of highest stress, the $3R$ structure is observed, which is con-

sistent with Martynov's observation that $3R$ is the product phase with the highest stress. Far away from the crack tip, where the stress is weak, the structure is the sevenfold-modulated microstructure characteristic of the β phase of this composition.⁸ Closer to the crack tip, the ordered $7M$ structure is observed which is the low-temperature zero-stress structure. At distances between the ordered $7M$ and the micromodulated β phase, another modulated β phase microstructure is observed, but with a wavelength of 5.3 [110] distances corresponding to a reciprocal-lattice distance of $\xi \sim 0.19$ along $[\xi\xi 0]$. The conclusion from this measurement is that the wave vector of the modulation increases with stress to a value of $\xi \sim 0.19$ for a stress just below that necessary to induce the ordered $7M$ structure. This is confirmed in the present experiment where the wave vector of the elastic scattering increases to $\xi \sim 0.18$ just below the transformation (Fig. 5) and the minimum in the dispersion curve also shifts to larger ξ values as the stress increases (Fig. 2).

The TA_2 phonons soften significantly when stress is applied. This is contrary to what would be expected from normal anharmonicity where one would expect the lattice to become stiffer and the energy to increase. This softening supports Clapp's localized soft-mode (LSM) theory for nucleation¹³ of martensite which we shall now discuss.

Nearly all martensite transformations are first order and no lattice dynamical mode becomes completely soft and thus drives the transition.¹⁰ Yet, the crystal appears to transform in a manner consistent with a homogeneous soft-mode behavior. The LSM is helpful in describing the nucleation processes occurring in the MT, since the regions where the elastic constants are small, are the nucleation sites for the product phase. The LSM theory was applied to the long-wavelength limit where elastic constants describe the dynamics but it can be extended to finite q values. It is assumed that a defect is present and a stress field exists about the defect that will drive the elastic constant to a small value in the localized region of the crystal. This can be seen by looking at the behavior of the elastic constants of a cubic crystal under uniaxial compression which has been described by the Thurston and Brugger:²⁵

$$\left(\frac{dC_0}{d\sigma} \right) = -t_\alpha t_\beta (q_\alpha q_\beta + 2C_0 S_{ij\alpha\beta} \epsilon_i \epsilon_j + C_{ijklmn} S_{m\alpha\beta} q_j \epsilon_i \epsilon_k), \quad (1)$$

where C_0 is the elastic constant, S_{ijkl} is the second-order elastic compliance, C_{ijklmn} is the third-order elastic constant, and \mathbf{t} is the unit vector of compression, \mathbf{q} is the unit vector of the propagation direction and ϵ is the polarization direction. For the case under consideration,^{26,27} $C_0 = C' = 1/2(C_{11} - C_{12})$, $\mathbf{q} = 1/\sqrt{2}[110]$, $\epsilon = 1/\sqrt{2}[1\bar{1}0]$, and $\mathbf{t} = [001]$, and the above equation simplified (using compressed notation) to

$$\left(\frac{dC'_\sigma}{d\sigma} \right) = 2C'S_{12} - \frac{1}{2}S_{12}C_{11} - \frac{1}{2}(S_{11} - S_{12})C_{112} + \frac{1}{2}S_{11}C_{123}, \quad (2)$$

which can be integrated and written simply as

$$C'_\sigma = C' - S\sigma, \quad (3)$$

where S depends upon the third-order elastic constants. These have only been measured for a very few materials, among them the martensitic alloy^{26,27} Cu-Zn-Al. If one substitutes the third-order elastic constants into Eq. (2) along with the second-order elastic constants, the quantity S is found to be positive so C' decreases with increasing σ for compression along [001].

Since we do not know the third-order elastic constants for $\text{Ni}_x\text{Al}_{1-x}$ we cannot predict how C'_σ will behave with stress. For the case of Cu-Zn-Al, where the third-order elastic constants have been measured, Verlinden and De-laey²⁷ have shown that C'_σ decreases by about 30% with a uniaxial compression of 300 MPa. They also demonstrated by the use of Eq. (1), that if an additional shear strain of a {110} $\langle 1\bar{1}0 \rangle$ type is added the elastic constant can actually go to zero. Now, in the region of a defect in a solid such as a local lattice deformation where the periodicity is disrupted, the strain field can be quite complicated and it is reasonable to have the proper components of the compression and shear strains that can cause C'_σ to soften *locally* in the region around the defect.

The LSM picture is consistent with the appearance of the phonon line shapes as shown in Fig. 3. It is clear that the linewidth increases as the stress increases [compare Fig. 3(d) with 3(e)]. This change in linewidth could be due to increased anharmonicity, but it can also be interpreted as a distribution of different phonon energies corresponding to different regions of the crystals where the shear strains are different. Since we are probing the

entire 125-mm³ volume, the different regions contribute to the overall spectra proportional to their volume. This type of inhomogeneous broadening could be the origin of the broadened spectra and clearly supports the LSM theory of Clapp.¹³

CONCLUSIONS

Uniaxial stress and temperature dramatically affect the [$\xi\xi 0$]-TA₂ phonon-dispersion branch in $\text{Ni}_{62.5}\text{Al}_{37.5}$. The ξ value of the phonon anomaly shifts to larger values with applied stress and a lowering of the temperature. This contrasts with stress measurements of the TA₂ branch on other alloys known to exhibit martensitic phases, namely, Cu-Al-Ni (Ref. 28) and Cu-Al-Pd (Ref. 29) where only a small (<10%) change in the branch is observed. Further experiments are planned to probe the low-temperature phase and the effects of stress and temperature on other compositions.

ACKNOWLEDGMENTS

The authors would like to thank P. C. Clapp, K. M. Ho, S. C. Moss, Y. Noda, L. E. Tanner, and Y. Yamada for the many stimulating discussions. One of us (S.M.S.) thanks the staffs at AECL, Chalk River, and LLB, Saclay for the hospitality while these experiments were being performed. Work at Brookhaven was supported by the Division of Materials Science, U.S. Department of Energy, under Contract No. DE-AC02-76CH00016. Portions of this work were carried out as part of the U.S.-Japan Collaboration on Neutron Scattering.

¹Z. Nishiyama, *Martensitic Transformations* (Academic, New York, 1978).
²L. E. Tanner and M. Wüttig, *Mater. Sci. Eng. A* **127**, 137 (1990).
³N. Rusovic and H. Warlimont, *Phys. Status Solidi A* **44**, 609 (1977).
⁴S. M. Shapiro, *Metall. Trans.* **12A**, 567 (1981); *Mater. Sci. Forum* **56-58**, 33 (1990).
⁵S. K. Satija, S. M. Shapiro, M. B. Salamon, and C. M. Wayman, *Phys. Rev. B* **29**, 6031 (1984).
⁶S. M. Shapiro, J. Z. Larese, Y. Noda, S. C. Moss, and L. E. Tanner, *Phys. Rev. Lett.* **57**, 3189 (1986).
⁷S. M. Shapiro, B. X. Yang, G. Shirane, J. Z. Larese, L. E. Tanner, and S. C. Moss, *Phys. Rev. Lett.* **62**, 1298 (1988).
⁸S. M. Shapiro, B. X. Yang, Y. Noda, L. E. Tanner, and D. Schryvers, *Phys. Rev. B* **44**, 9301 (1991).
⁹N. Nakanishi, *Prog. Mater. Sci.* **24**, 143 (1979).
¹⁰J. Krumhansl and R. J. Gooding, *Phys. Rev. B* **39**, 3047 (1989).
¹¹A. G. Khachatryan, *Theory of Structural Transformations in Solids* (Wiley, New York, 1983).
¹²G. B. Olson and M. Cohen, *Metall. Trans. A* **7**, 1897 (1976); **7**, 1905 (1976); **7**, 1915 (1976).
¹³P. C. Clapp, *Phys. Status Solidi B* **57**, 561 (1973); *Mater. Sci. Eng.* **38**, 193 (1979); **A 127** (1990).
¹⁴G. Guenin and P. C. Clapp, *Proceedings of the International*

Conference on Martensitic Transformations (ICOMAT-86) (Japan Institute of Metals, Sendai, 1986), p. 171.
¹⁵M. F. Singleton, J. L. Murray, and P. Nash, in *Binary Alloy Phase Diagrams*, edited by T. B. Massalski (American Society for Metals, Metals Park, OH, 1986), p. 140.
¹⁶S. Chakravorty and C. M. Wayman, *Metall. Trans. A* **7**, 555 (1976); **7**, 569 (1976); K. Enami, S. Nenno, and K. Shimizu, *Trans. Jpn. Inst. Met.* **14**, 161 (1973); K. Enami, A. Nagasawa, and S. Nenno, *Scr. Metall.* **12**, 223 (1978).
¹⁷S. Ochiai and M. Ueno, *Trans. Jpn. Inst. Met.* **52**, 157 (1988).
¹⁸Y. Noda, S. M. Shapiro, G. Shirane, Y. Yamada, K. Fuchizaki, and L. E. Tanner, *Mater. Sci. Forum* **56-58**, 299 (1990); *Phys. Rev. B* **42**, 10397 (1990).
¹⁹L. E. Tanner, A. R. Pelton, and R. Gronsky, *J. Phys. (Paris) Colloq.* **43**, C4-169 (1982).
²⁰C. Zener, *Phys. Rev.* **71**, 846 (1947).
²¹A. Draperi and C. Vettier, *Rev. Phys. Appl.* **19**, 823 (1984).
²²V. V. Martynov, K. Enami, L. G. Khandros, S. Nenno, and A. V. Tkachenko, *Fiz. Met. Metalloved.* **55**, 982 (1983) [*Phys. Met. Metallogr. (USSR)* **55**(5), 136 (1983)]; *Scr. Metall.* **17**, 1167 (1983).
²³C. Zhao and B. N. Harmon, *Phys. Rev. B* **45**, 2818 (1992).
²⁴D. Schryvers and L. E. Tanner, in *Shape-Memory Materials and Phenomena-Fundamental Aspects and Applications*, edited by C. T. Liu, M. Wüttig, K. Otsuka, and H. Kunsmann, MRS Symposia Proceedings No. 246 (Materials Research So-

- ciety, Pittsburgh, 1992), p. 33.
- ²⁵R. N. Thurston and K. Brugger, *Phys. Rev.* **133**, 1604 (1964).
- ²⁶G. Guenin and P. F. Gobin, *Metall. Trans. A* **13A**, 1127 (1982).
- ²⁷B. Verlinden and L. Delaey, *J. Phys. F* **16**, 1391 (1986); *Metall. Trans.* **19A**, 207 (1988).
- ²⁸H. Tanahashi, Y. Mori, M. Iizumi, T. Suzuki, and K. Otsuka, *Proceedings of the International Conference on Martensitic Transformations (ICOMAT-86)* (Japan Institute of Metals, Sendai, 1986), p. 207.
- ²⁹A. Nagasawa, A. Kuwabara, Y. Morii, K. Fuchizaki, and S. Funahashi, *Mater. Trans. (JIM)* **33**, 203 (1992).